Published in final edited form as:
J Hepatol. 2012 September ; 57(3): 577–583. doi:10.1016/j.jhep.2012.04.026.

Inactivation of Spry2 accelerates AKT-driven hepatocarcinogenesis via activation of MAPK and PKM2 pathways

Chunmei Wang[1,#], **Salvatore Delogu**[2,#], **Coral Ho**[1], **Susie A. Lee**[1], **Bing Gui**[1], **Lijie Jiang**[1], **Sara Ladu**[3], **Antonio Cigliano**[2], **Frank Dombrowski**[2], **Matthias Evert**[2], **Diego F. Calvisi**[2], and **Xin Chen**[1,4,*]

[1]Department of Bioengineering and Therapeutic Sciences, University of California, San Francisco, USA

[2]Institute of Pathology, University of Greifswald, Greifswald, Germany

[3]Department of Medicine and Aging, University of Chieti, Chieti, Italy

[4]Liver Center, University of California, San Francisco, USA

Abstract

Background & Aims—Aberrant activation of the AKT oncogenic pathway and downregulation of the Sprouty 2 (*Spry2*) tumor suppressor gene are frequently observed molecular events in human hepatocarcinogenesis. The goal of the present study was to investigate the eventual biochemical and genetic crosstalk between activated AKT and inactivation of Spry2 during liver cancer development by using *in vivo* and *in vitro* approaches.

Methods—Activated *AKT* and/or *Spry2Y55F*, a dominant negative form of *Spry2*, were overexpressed in the mouse liver via hydrodynamic gene delivery. Histological and biochemical assays were applied to characterize the molecular features of AKT and AKT/Spry2Y55F liver tumors. The human HLE hepatocellular carcinoma (HCC) cell line, stably overexpressing *AKT*, was transfected with *Spry2Y55F* to study the molecular mechanisms underlying hepatocarcinogenesis driven by Spry2 loss.

Results—*Spry2Y55F* overexpression significantly accelerated AKT induced hepatocarcinogenesis in the mouse. AKT/Spry2Y55F liver lesions had increased proliferation and glycolysis and decreased lipogenesis when compared with AKT corresponding lesions. At the molecular level, AKT/Spry2Y55F HCCs exhibited a significantly stronger induction of activated mitogen-activated protein kinase (MAPK) and Pyruvate Kinase M2 (PKM2) pathways than in AKT corresponding lesions. This phenotype was reproduced in HLE cells overexpressing *AKT* following transfection with *Spry2Y55F*. Furthermore, we found that concomitant suppression of the MAPK cascade and PKM2 strongly inhibited the growth induced by Spry2Y55F in *AKT*-overexpressing cells.

[*]**Corresponding author:** UCSF, 513 Parnassus Ave., San Francisco, CA 94143, U.S.A. Tel: (415) 502-6526; Fax: (415) 502-4322; xin.chen@ucsf.edu. .
[#]These authors contributed equally to this work.

The Authors declare no conflict of interest.

Conclusions—Inactivation of Spry2 accelerates AKT induced hepatocarcinogenesis via activation of MAPK and PKM2 pathways.

Keywords

HCC; AKT; Spry2; MAPK; PKM2

Introduction

Human hepatocellular carcinoma (HCC) is the third most common cause of cancer death worldwide [1]. Treatment options for HCC are limited. Sorafenib, a multikinase inhibitor, is the only available drug that significantly increases the survival of patients with advanced HCC [2-4]. To develop more effective therapies against HCC, a better understanding of the molecular mechanisms underlying HCC development is required [2, 4, 5].

HCC development is a multi-step process in which multiple pathways are deregulated [2, 4, 5]. Among them, the v-akt murine thymoma viral oncogene homolog (AKT)/ mammalian target of rapamycin (mTOR) cascade is a one of the most frequently activated pathways [5,6]. AKT exerts many of its cellular effects through its key downstream effector, the mTOR complex 1 (mTORC1) [6, 7]. Accordingly, the mTORC1 axis is also frequently activated in human HCC [8]. Generally, the phosphorylation of ribosomal protein S6 (RPS6) is used as a surrogate marker for mTORC1 activation [9]. The importance of the AKT pathway in hepatocarcinogenesis has been recently further substantiated by our group. Noticeably, we found that overexpression of an activated form of AKT in the mouse liver induces lipogenesis as well as hepatocyte proliferation, eventually leading to liver tumor formation within six months [10]. Similar results were previously obtained in mice depleted of the AKT specific inhibitor, phospatase and tensin homolog [11].

The Ras/mitogen-activated protein kinase (MAPK) signaling is another aberrantly activated pathway in human HCC [12]. However, Ras or Raf mutations are extremely rare in HCC, implying that activation of the Ras/MAPK cascade occurs in a context of wild-type Ras and Raf in this disease [13, 14]. Sprouty 2 (Spry2), one of the Sprouty family members evolutionarily conserved inhibitors of receptor tyrosin kinases, negatively regulates the Ras/MAPK pathway [15]. Expression of Spry2 protein is frequently downregulated and its loss is significantly associated with activation of the Ras/MAPK pathway in HCC [16-18]. Furthermore, inactivation of Spry2 via Spry2Y55F, a dominant negative form of Spry2, cooperates with other activated oncogenic proteins, such as β-catenin or c-Met, to induce HCC development in mice [18, 19].

The possible crosstalk between the AKT/mTOR and Ras/MAPK pathways during hepatocarcinogenesis is suggested by the recent finding that co-expression of activated AKT and mutated N-Ras rapidly induces HCC development in mice [20]. To further investigate the interaction(s) between these two pathways during hepatocarcinogenesis and to better reproduce the human disease, in which the Ras genes are not mutated [13, 14], we co-expressed an activated/myristoylated form of *AKT* (*myr-AKT*) and *Spry2Y55F* in the mouse liver by hydrodynamic injection. Our data show that loss of Spry2 synergizes with AKT activation to induce rapid hepatocarcinogenesis through the activation of MAPK and PKM2 pathways.

Materials and Methods

Constructs and reagents

The constructs used for mouse injection, including pT3-EF1α-HA-myr-AKT, pT3-EF1α-Spry2Y55F-V5, and pCMV/sleeping beauty transposase (SB), were described previously [10, 18, 21]. Plasmids were purified using the Endotoxin free Maxi prep kit (Sigma, St. Louis, MO).

Hydrodynamic injection and mouse monitoring

Wild-type FVB/N mice were obtained from Charles River (Wilmington, MA). Hydrodynamic injections were performed as described previously [10, 18, 21]. Briefly, ten micrograms of the plasmids encoding *myr-AKT* and/or *Spry2Y55F* along with sleeping beauty transposase in a ratio of 25:1 were diluted in 2 mL saline (0.9% NaCl) for each mouse. Saline solution was filtered through a 0.22 μm filter and injected into the lateral tail vein of 6 to 8-week-old FVB/N mice in 5 to 7 seconds. Mice were housed, fed, and monitored in accordance with protocols approved by the committee for animal research at the University of California, San Francisco.

Histology and immunohistochemistry

Livers were fixed in 4% paraformaldehyde and processed for paraffin embedding. Preneoplastic and neoplastic liver lesions were assessed by two board-certified pathologists (M.E. and F.D.) in accordance with the criteria by Frith et al. [22]. Immunohistochemistry was performed, and proliferation and apoptotic indices were determined, as described [20].

Metabolic parameters measurement

Fatty acid synthesis was measured by incorporation of [U-^{14}C] acetate into lipids. Liver lysates were labelled with [U-^{14}C] acetate. Lipids were Folch extracted and counted for ^{14}C. Hepatic cholesterol and lactate content was assessed with the Cholesterol Quantification and the Lactate Assay Kit II (BioVision Inc., Mountain View, CA), respectively, following the manufacturer's protocol.

Immunoblotting and kinase assays

Murine hepatic tissues were processed as described in Supplementary Materials. Nitrocellulose membranes were probed with specific primary antibodies (Supplementary Table 1). AKT and MAPK kinase activities were assessed with the AKT and p44/42 MAPK kinase assay kits (Cell Signaling Technology, Danvers, MA), respectively, following the manufacturer's protocol.

Cell line

The human HCC cell line HLE was used for the *in vitro* experiments. This cell line expresses low AKT levels and does not harbor β-catenin mutations. Transfection with cDNA and siRNAs and treatment with inhibitors were performed as described in Supplementary Materials.

Statistical analysis

Tukey-Kramer test was used to evaluate statistical significance. Values of $P < 0.05$ were considered significant. Data are expressed as means ± SD.

See Supplementary Materials for more detailed descriptions of Materials and Methods.

Results

Spry2Y55F accelerates AKT induces liver tumor development in mice

To determine whether down-regulation of Spry2 cooperates with activated AKT to induce hepatocarcinogenesis, we co-injected HA-tagged *myr-AKT* and V5-tagged *Spry2Y55F*, a dominant negative form of Spry2 [18, 19], along with the sleepy beauty transposase, into the mouse liver by hydrodynamic injection. In accordance with our previous studies, we found that overexpression of *Spry2Y55F* alone (n = 10) did not lead to histological abnormalities 6 months post-injection [18, 19], whereas overexpression of *myr-AKT* resulted in hepatocellular adenoma (HCA) and HCC development by 3 and 6 months post-injection, respectively [10]. Noticeably, following co-injection of *myr-AKT* and *Spry2Y55F* (which will be referred to as AKT/Spry2Y55F mouse in this paper), AKT/Spry2Y55F mouse livers became larger, spotted and paler around 6 weeks post-injection (Fig. 1A). Eight weeks after hydrodynamic injection, liver nodules developed in AKT/Spry2Y55F mice (Fig. 1A). Large, palpable liver tumors were observed in 4 of 5 AKT/Spry2Y55F mice after 14 weeks post-injection, while AKT mice did not develop any nodule at this time point (Fig. 1A and Supplementary Fig. 1) [10]. AKT/Spry2Y55F mice developed large tumors and required to be euthanized by 21 weeks post-injection (Fig. 1B).

Histologically, 6 weeks post-injection, preneoplastic lesions occupied 50-60% of the hepatic parenchyma but no tumors were present (Fig. 2A, upper panel). Preneoplastic lesions formed clusters of cells in the acinar zone 3 surrounding the hepatic veins. Lesion cells stored elevated amounts of glycogen (as indicated by positive PAS reaction) and lipids (Fig. 2A, lower panel). Mallory-Denk-bodies were occasionally found in these cells (Fig. 2A, arrow). Importantly, preneoplastic cells expressed both the HA-tag of AKT and the V5-tag of Spry2Y55F, while the surrounding normal hepatocytes were negative for HA-tag and V5-tag staining (Fig. 3A). This specific immunohistochemical pattern indicates that only the cells that incorporated the hydrodynamically injected plasmids were morphologically altered. Only a few lesions expressed activated/phosphorylated extracellular-related kinase (p-ERK) proteins (Fig. 3A). Eight weeks post-injection, the amount of preneoplastic lesions did not increase significantly, but hepatocellular adenomas and small HCCs started to emerge (Fig. 1A, 2B). Furthermore, some neutrophil granulocytes infiltrated small areas of all tumors. Some of these granulocytes were ingested by the neoplastic hepatocytes, as indicated by Naphthol AS-D Chloroacetate (CLAE) staining (Fig. 2B, lower middle panel**).** This phenomenon is called emperipolesis, a feature which can be occasionally observed in human HCC [23]. Most granulocytes underwent apoptosis after emperipolesis, as indicated by TUNEL assay (Fig. 2B, lower right panel). Importantly, all tumors at this and later stages expressed both HA- and V5-tag, further underlying that tumor development only took place in genetically modified cells (Fig. 3B and Supplementary Fig. 2). Moreover, all tumors at this and later stages strongly expressed p-ERK in both nuclei and cytoplasm (Fig. 3B), indicating that the neoplastic transformation is closely related to sustained activation of the MAPK signalling. Ten weeks post-injection (data not shown), the amount of preneoplastic tissue increased and occupied 80-90% of the entire non-tumorous liver. Many large HCCs up to 10 mm in diameter developed in AKT/Spry2Y55F mouse livers. Emperipolesis was detected in some areas of these HCCs. In addition, a mild fibrotic reaction was observed in AKT/Spry2Y55F liver tumors, particularly in large HCCs. The HCCs further progressed in size and reached up to 20 mm in diameter 14 weeks post-injection (Fig. 2C). The large HCCs displayed confluent areas of necrosis, an increase in cytologic atypia, and a significant loss of lipid content when compared to the preneoplastic lesions and small HCCs developed 8 weeks post-injection (Fig. 2C). Emperipolesis and a mild fibrotic phenotype were also common features of AKT/Spry2Y55F liver lesions at this time point. Several HCCs larger than 20 mm were present at later time points and were frequently confluent

(data not shown). Different from AKT mice, no lesions with cholangiocellular/ductular differentiation were detected in AKT/Spry2Y55F livers at all time points. Altogether, these results demonstrate that loss of Spry2 accelerates AKT induced hepatocarcinogenesis in mice.

Proliferation and glycolysis are increased in AKT/Spry2Y55F liver tumors

To elucidate the cellular mechanisms responsible for accelerated hepatocarcinogenesis in AKT/Spry2Y55F mice, we compared the proliferation, apoptosis and angiogenesis indices in wild-type livers, Spry2Y55F mice livers, and preneoplasia and HCCs from AKT and AKT/Spry2Y55F mice. Proliferation, apoptosis and angiogenesis indices were significantly higher in preneoplasia and HCC of AKT and AKT/Spry2Y55F mice than in wild-type and Spry2Y55F livers (Supplementary Fig. 3A-C). The proliferation rate was highest in AKT/Spry2Y55F HCCs and significantly higher in AKT/Spry2Y55F preneoplastic lesions than in corresponding AKT lesions. Apoptosis rate in preneoplastic lesions and HCCs of AKT and AKT/Spry2Y55F mice did not show significant differences. Angiogenesis degree in AKT and AKT/Spry2Y55F HCCs was similar, and significantly higher than that in AKT and AKT/Spry2Y55F preneoplastic lesions. These results suggest that the increase of cell proliferation represents the major mechanism triggered by loss of Spry2 activity in accelerating AKT induced hepatocarcinogenesis.

Altered cell metabolism, especially consisting of increased glycolysis and lipogenesis, is a hallmark of tumorigenesis [24]. For instance, AKT can induce lipogenesis and eventually lead to HCC development [10]. To determine the role of the lipid and glucose metabolism in hepatocarcinogenesis induced by *AKT* overexpression either alone or in combination with *Spry2Y55F*, we analyzed the fatty acid (FA) synthesis, cholesterol content, and lactate content in wild-type livers, Spry2Y55F livers, preneoplasia and HCCs of AKT and AKT/Spry2Y55F mice (Supplementary Fig. 3D-F). The three parameters were significantly higher in AKT and AKT/Spry2Y55F preneoplasia and HCCs when compared with wild-type livers. Both FA synthesis and cholesterol content were equivalent in AKT and AKT/Spry2Y55F preneoplastic livers. FA synthesis and cholesterol content further increased in AKT HCCs, whereas the same parameters declined in AKT/Spry2Y55F HCCs and were significantly lower than those in AKT and AKT/Spry2Y55F preneoplastic lesions. These results indicate that lipogenesis plays an important role at the early but not the late stage of AKT/Spry2Y55F hepatocarcinogenesis. Lactate is a major product of tumor cell aerobic glycolysis [25]. The lactate content was similar in AKT and AKT/Spry2Y55F preneoplastic lesions. The lactate content remarkably increased in AKT/Spry2Y55F HCCs and was significantly higher than that of the other groups. These results suggest that increased cell glycolysis might be a mechanism whereby loss of Spry2 contributes to accelerate AKT HCC development.

MAPK pathway and the master glycolysis regulator PKM2 are upregulated in AKT/Spry2Y55F HCC

Next, to investigate the molecular downstream pathways mediating AKT/Spry2Y55F induced hepatocarcinogenesis, we analyzed the expression levels of some of the major signaling cascades in AKT and AKT/Spry2Y55F HCCs.

Expression levels of activated/phosphorylated AKT, activated/phosphorylated mTOR (a major downstream effector of AKT), and mTOR targets, including activated/phosphorylated RPS6, VEGF-α, and the pro-lipogenic proteins SREBP1, SREBP2, FASN, and SCD1 were highest in AKT HCCs (Fig. 4A and Supplementary Fig. 4). Kinase assay further confirmed that the AKT kinase activity was lower in AKT/Spry2Y55F HCCs than that in AKT tumors (Fig. 4B). These results were consistent with the finding that lipogenesis, a dominant feature

of activated AKT/mTOR pathway [10], was lower in AKT/Spry2Y55F liver tumors than in AKT HCCs. By contrast, levels of p-ERK and its downstream target, activated/phosphorylated ELK1, were much higher in AKT/Spry2Y55F liver tumors than in AKT corresponding lesions (Fig. 4A). Kinase assay also confirmed that the kinase activity of MAPK was significantly higher in AKT/Spry2Y55F than in AKT liver tumors (Fig. 4C). Furthermore, AKT/Spry2Y55F HCCs showed strongest activation of the epidermal growth factor receptor (EGFR) and fibroblast growth factor receptor (FGFR) cascades, as shown by increased levels of total and activated/phosphorylated EGFR and activated/phosphorylated FGFR substrate 2 (FRS2), when compared with AKT tumors (Fig. 4A and Supplementary Fig. 4). The same differences in activation of the AKT/mTOR and ERK cascades were detected in preneoplastic lesions (Supplementary Fig. 5), indicating that specific molecular alteration occur early in AKT/Spry2Y55F-driven hepatocarcinogenesis.

To study the molecular mechanism leading to the increased glycolysis in AKT/Spry2Y55F tumors, we assayed some of the key glycolysis proteins as well as major regulators of glycolysis in the mouse sample collection. We found that the expression level of PKM2, the master regulator of glycolysis [25], was remarkably highest in AKT/Spry2Y55F HCCs, which was also confirmed by immunohistochemical staining (Supplementary Fig. 6). Induction of glycolysis was also underscored by the highest levels of membranous translocation of glucose transporters (GLUT) 1 and 4 in AKT/Spry2Y55F HCCs. On the other hand, expression levels of hexokinase II and aldolase A were equivalent in AKT/Spry2Y55F and AKT HCCs (Fig. 4A and Supplementary Fig. 4). Unexpectedly, the expression of c-Myc and HIF1α, both considered to be the main regulators of glycolysis and PKM2 [25], was comparable in AKT and AKT/Spry2Y55F HCCs. Altogether, the data indicate that accelerated hepatocarcinogenesis in AKT/Spry2Y55F mice is associated with induction of the MAPK pathway and elevated glycolysis.

Loss of Spry2 induces cell growth via MAPK and PKM2 pathways

To further elucidate the molecular mechanisms underlying loss of Spry2 and activated AKT signaling in promoting hepatocarcinogenesis, we utilized the HLE cell line stably transfected with *AKT*. After transfection, HLE cells display elevated levels of AKT while the activation degree of ERK proteins was unaffected (Supplementary Fig. 7). HLE cells were then transiently transfected with *Spry2Y55F*. Consistent with the *in vivo* results, overexpression of *Spry2Y55F* significantly increased cell proliferation, while a slight decrease of apoptosis was detected 48 hours after transfection (Supplementary Fig. 8B and C). At the molecular level, overexpression of *Spry2Y55F* was accompanied by upregulation of MAPK, EGFR, and FGFR pathways as well as of PKM2, and membranous GLUT1 and GLUT4 proteins, two additional markers of glycolysis (Supplementary Fig. 8A). To define the specific contribution of the MAPK and AKT/mTOR pathways in the growth of HLE cells transfected with AKT and Spry2Y55F, cells were treated with UO126, a MEK inhibitor, or NVP/BEZ235, a dual PI3K/mTOR inhibitor. As expected, UO126 decreased the expression of p-ERK and p-ELK1, whereas NVP/BEZ235 inhibited the expression of p-AKT and p-RPS6 (Supplementary Fig. 8A). Noticeably, UO126 inhibited proliferation and induced apoptosis in AKT/Spry2Y55F transfected HLE cells much more efficiently than NVP/BEZ235 (Supplementary Fig. 8B and C). At the metabolic level, UO126 treatment resulted in a stronger lowering effect on glycolysis and a less pronounced decrease in lipogenesis than NVP/BEZ235 did (Supplementary Fig. 9). UO126 treatment also decreased the expression levels of EGFR, p-EGFR and p-FRS2, suggesting that activation of EGFR and FGFR pathways is MAPK-dependent in AKT/Spry2Y55F tumor cells. Furthermore, levels of GLUT1 and GLUT4 were more significantly inhibited by UO126 than NVP/BEZ235 treatment. Interestingly, neither UO126 nor NVP/BEZ235 treatment inhibited

PKM2 expression in HLE cells, implying that PKM2 activation induced by Spry2Y55F is independent of MAPK or AKT/mTOR cascades.

Since Spry2 is able to suppress the activation of the ERK cascade through the inhibition of EGFR- and FRS2-mediated activation of the ERK proteins [15], we assessed the consequence of inactivating EGFR and/or FRS2 in HLE cells. Silencing of either EGFR or FRS2 by siRNA significantly reduced both the activation of ERK proteins and the growth of HLE cells transfected with AKT and Spry2Y55F. Of note, combined suppression of EGFR and FRS2 led to a stronger growth restraint and reduction of activation of ERK proteins when compared with silencing of EGFR or FRS2 alone (Supplementary Fig. 10). These data imply a prominent role of EGFR and FRS2 in the activation of ERK in this cell line.

Finally, we investigated whether concomitant suppression of MAPK and PKM2 can synergistically inhibit AKT/Spry2Y55F tumor cell proliferation. For this purpose, HLE cells transfected with AKT and Spry2Y55F were treated with UO126 and/or PKM2 siRNA. Both UO126 treatment and PKM2 siRNA alone were capable of inhibiting the cell growth in AKT/Spry2Y55F transfected HLE cells. Combined treatment of UO126 and PKM2 siRNA resulted in a much more pronounced growth inhibition of HLE cells when compared with single treatments (Supplementary Fig. 11B and C). Of note, the combined treatment resulted in a synergistic anti-glycolytic effect, while it did not further lower the levels of fatty acid synthesis in HLE cells (Supplementary Fig. 12). Marked reduction of glycolysis by the combination of UO126 and PKM2 siRNA was also underscored by the complete suppression of GLUT1 and GLUT4 membranous localization (Supplementary Fig. 11A). Altogether, the *in vitro* studies indicate that MAPK and PKM2 pathways independently contribute to AKT/Spry2Y55F induced hepatocarcinogenesis.

Activation of PKM2 is independent of c-Myc in AKT/Spry2Y55F liver tumors

A previous study showed that PKM2 activation is c-Myc dependent in gliomas [26]. To determine whether c-Myc expression accounts for the upregulation of PKM2 in AKT/Spry2Y55F HCCs, HLE cells overexpressing AKT and Spry2Y55F were subjected to c-Myc silencing via siRNA. However, c-Myc siRNA did not inhibit the expression of PKM2 (Supplementary Fig. 13), indicating that PKM2 activation in the AKT/Spry2Y55F tumor cells is independent of c-Myc.

Discussion

In this study, we show that inactivation of the Ras/MAPK inhibitor, Spry2, cooperates with AKT to induce rapid hepatocarcinogenesis in the mouse. Intriguingly, we found that co-expression of Spry2Y55F and AKT results in the development of liver tumors exhibiting unique morphological, metabolic, and molecular features.

At the morphological level, AKT/Spry2Y55F preneoplasia and HCC consisted exclusively of lesions with hepatocytic differentiation. In contrast, we previously showed that AKT mice developed liver lesions with hepatocytic, ductular or mixed differentiation [25]. These data imply that loss of Spry2 promotes the development of liver lesions characterized by a commitment toward the hepatocyte lineage. Since AKT/Ras mice also exhibit lesions with a ductular differentiation [25], the present data imply that suppression of Spry2 drives the liver lesions toward hepatocytic differentiation independent of its inhibitory effect on the Ras/MAPK pathway. In addition, only HCCs from Spry2Y55F/AKT mice showed features of emperipolesis. This phenomenon, consisting of the presence of cells within the cytoplasm of another cell, mainly of cancerous nature, remains poorly understood and requires additional investigation. Nevertheless, the present findings indicate that Spry2 might represent an important regulator of emperipolesis in the cell.

At the molecular level, loss of Spry2 expression resulted in upregulation of ERK/MAPK, EGFR, and FGFR cascades in *AKT*-overexpressing livers. In particular, our data show that the activation of the EGFR and FGFR pathways depends on the ERK/MAPK cascade. Since the latter pathways are all able to induce the ERK/MAPK signaling, the present data suggest that loss of Spry2 amplifies the magnitude of ERK/MAPK cascade by inducing a positive feed-back loop that activates the upstream inducers of ERK. Furthermore, we found that Spry2Y55F upregulates the master regulator of glycolysis, PKM2. The importance of the ERK/MAPK and PKM2 pathways on AKT/Spry2Y55F growth is underscored by subsequent experiments conducted in HLE HCC cells, in which concomitant suppression of ERK/MAPK and PKM2 resulted in a striking inhibition of cell growth. Based on these data, it is tempting to speculate that liver tumor cells expressing high levels of AKT and low levels of Spry2 are specifically addicted to ERK/MAPK and PKM2 cascades. Thus, concomitant inhibition of the ERK/MAPK and PKM2 pathways might represent a promising therapeutic approach in HCC (and other tumor types) characterized by overexpression of AKT and loss of Spry2.

To the best of our knowledge, this is the first report showing that PKM2 is downregulated by Spry2. Previous studies showed that PKM2 plays an important role in tumor metabolism by providing ATP for cell proliferation [25, 27, 28] and activating other oncogenes, such as β-catenin [29]. In particular, it has been reported that EGFR activation induces nuclear translocation of PKM2 in brain tumors. Once in the nucleus, PKM2 activates β-catenin, leading to cell proliferation and tumorigenesis [29]. However, AKT/Spry2Y55F HCCs did not show activation of the WNT/β-catenin cascade (Supplementary Fig. 14). Nevertheless, it is of high interest that hepatocarcinogenesis induced by overexpression of either mutant β-catenin [30] or AKT (this study) in association with Spry2Y55F led to similar cellular and molecular alterations, including augmented proliferation and activation of the ERK pathway. These data suggest that inactivation of Spry2 might predominantly contribute to hepatocarcinogenesis driven by different signaling cascades by promoting proliferation and activating the ERK pathway. In addition, when EGFR upregulation was downregulated by in AKT/Spry2Y55F cells, we observed that the upregulation of PKM2 was not affected. It has been demonstrated that PKM2 is upregulated either by the c-Myc transcription factor [26] or HIF-1α in several tumor types [30]. Unexpectedly, in our *in vivo* and *in vitro* systems, we found that PKM2 was upregulated independent of c-Myc and AKT/mTOR (the upstream inducer of HIF-1α). Also, liver lesions from AKT/Ras mice, characterized by a high degree of activation of mTOR, c-Myc, HIF-1α, and MAPK activation [30], showed low levels of PKM2 (data not shown). Thus, PKM2 upregulation by Spry2Y55F is independent of c-Myc, MAPK, EGFR or HIF-1α in *AKT*-overexpressing cells. Although the mechanism(s) whereby Spry2 loss promotes PKM2 upregulation remains unknown, the lack of interaction between Spry2 and PKM2, as assessed by immunoprecipitation (Calvisi DF et al., unpublished observation), suggests that Spry2 effect on PKM2 is indirect. Additional studies are required to identify the intermediate proteins linking Spry2 to PKM2.

In summary, we showed that inactivation of Spry2 synergizes with AKT to rapidly induce hepatocarcinogenesis in the mouse. The major cellular and molecular mechanisms resulting from such collaboration are the strong activation of the MAPK pathway and the induction of glycolysis, to which the tumor cells with activated AKT and low Spry2 are addicted. Thus, the present findings unravel a crosstalk between Spry2 and AKT and envisage the possibility of implementing therapeutic approaches aiming at inhibiting MAPK and PKM2 pathways in HCC with inactivated Spry2 and elevated AKT.

Supplementary Material

Refer to Web version on PubMed Central for supplementary material.

Acknowledgments

Grant support: This work was supported by NIH grants R21CA131625 and R01CA136606 to XC; P30DK026743 for UCSF Liver Center; the Deutsche Forschungsgemeinschaft DFG (grant number Do622/2-1 and Ev168/2-1) to FD and ME.

Abbreviations

AKT	v-akt murine thymoma viral oncogene homolog
ERK	extracellular-related kinase
GLUT	glucose transporter
HCC	hepatocellular carcinoma
MAPK	mitogen-activated protein kinase
mTOR	mammalian target of rapamycin
mTORC	mTOR complex
RPS6	ribosomal protein S6
Spry2	Sprouty2
PKM2	pyruvate kinase M2

References

[1]. Parkin DM, Bray F, Ferlay J, Pisani P. Global cancer statistics, 2002. CA Cancer J Clin. 2005; 55:74–108. [PubMed: 15761078]

[2]. Llovet JM, Bruix J. Molecular targeted therapies in hepatocellular carcinoma. Hepatology. 2008; 48:1312–1327. [PubMed: 18821591]

[3]. Llovet JM, Ricci S, Mazzaferro V, Hilgard P, Gane E, Blanc JF, et al. Sorafenib in advanced hepatocellular carcinoma. N Engl J Med. 2008; 359:378–390. [PubMed: 18650514]

[4]. Villanueva A, Llovet JM. Targeted therapies for hepatocellular carcinoma. Gastroenterology. 2011; 140:1410–1426. [PubMed: 21406195]

[5]. Whittaker S, Marais R, Zhu AX. The role of signaling pathways in the development and treatment of hepatocellular carcinoma. Oncogene. 2011; 29:4989–5005. [PubMed: 20639898]

[6]. Manning BD, Cantley LC. AKT/PKB signaling: navigating downstream. Cell. 2007; 129:1261–1274. [PubMed: 17604717]

[7]. Zoncu R, Efeyan A, Sabatini DM. mTOR: from growth signal integration to cancer, diabetes and ageing. Nat Rev Mol Cell Biol. 2011; 12:21–35. [PubMed: 21157483]

[8]. Villanueva A, Chiang DY, Newell P, Peix J, Thung S, Alsinet C, et al. Pivotal role of mTOR signaling in hepatocellular carcinoma. Gastroenterology. 2008; 135:1972–1983. e1971–1911. 1983. [PubMed: 18929564]

[9]. Ruggero D, Sonenberg N. The Akt of translational control. Oncogene. 2005; 24:7426–7434. [PubMed: 16288289]

[10]. Calvisi DF, Wang C, Ho C, Ladu S, Lee SA, Mattu S, et al. Increased lipogenesis, induced by AKT-mTORC1-RPS6 signaling, promotes development of human hepatocellular carcinoma. Gastroenterology. 2010; 140:1071–1083. [PubMed: 21147110]

[11]. Galicia VA, He L, Dang H, Kanel G, Vendryes C, French BA, et al. Expansion of hepatic tumor progenitor cells in Pten-null mice requires liver injury and is reversed by loss of AKT2. Gastroenterology. 2010; 139:2170–2182. [PubMed: 20837017]

[12]. Calvisi DF, Ladu S, Gorden A, Farina M, Conner EA, Lee JS, et al. Ubiquitous activation of Ras and Jak/Stat pathways in human HCC. Gastroenterology. 2006; 130:1117–1128. [PubMed: 16618406]

[13]. Tsuda H, Hirohashi S, Shimosato Y, Ino Y, Yoshida T, Terada M. Low incidence of point mutation of c-Ki-ras and N-ras oncogenes in human hepatocellular carcinoma. Jpn J Cancer Res. 1989; 80:196–199. [PubMed: 2542205]

[14]. Challen C, Guo K, Collier JD, Cavanagh D, Bassendine MF. Infrequent point mutations in codons 12 and 61 of ras oncogenes in human hepatocellular carcinomas. J Hepatol. 1992; 14:342–346. [PubMed: 1323601]

[15]. Edwin F, Anderson K, Ying C, Patel TB. Intermolecular interactions of Sprouty proteins and their implications in development and disease. Mol Pharmacol. 2009; 76:679–691. [PubMed: 19570949]

[16]. Lo TL, Fong CW, Yusoff P, McKie AB, Chua MS, Leung HY, et al. Sprouty and cancer: the first terms report. Cancer Lett. 2006; 242:141–150. [PubMed: 16469433]

[17]. Fong CW, Chua MS, McKie AB, Ling SH, Mason V, Li R, et al. Sprouty 2, an inhibitor of mitogen-activated protein kinase signaling, is down-regulated in hepatocellular carcinoma. Cancer Res. 2006; 66:2048–2058. [PubMed: 16489004]

[18]. Lee SA, Ho C, Roy R, Kosinski C, Patil MA, Tward AD, et al. Integration of genomic analysis and in vivo transfection to identify sprouty 2 as a candidate tumor suppressor in liver cancer. Hepatology. 2008; 47:1200–1210. [PubMed: 18214995]

[19]. Lee SA, Ladu S, Evert M, Dombrowski F, De Murtas V, Chen X, et al. Synergistic role of Sprouty2 inactivation and c-Met up-regulation in mouse and human hepatocarcinogenesis. Hepatology. 2010; 52:506–517. [PubMed: 20683950]

[20]. Ho C, Wang C, Mattu S, Destefanis G, Ladu S, Delogu S, et al. AKT and N-Ras coactivation in the mouse liver promotes rapid carcinogenesis by way of mTOR, FOXM1/SKP2, and c-Myc pathways. Hepatology. 2012; 55:833–845. [PubMed: 21993994]

[21]. Carlson CM, Frandsen JL, Kirchhof N, McIvor RS, Largaespada DA. Somatic integration of an oncogene-harboring Sleeping Beauty transposon models liver tumor development in the mouse. Proc Natl Acad Sci U S A. 2005; 102:17059–17064. [PubMed: 16286660]

[22]. Frith CH, Ward JM, Turusov VS. Tumours of the liver. IARC Sci Publ. 1994; 223:269.

[23]. Xia P, Wang S, Guo Z, Yao X. Emperipolesis, entosis and beyond: dance with fate. Cell Res. 2008; 18:705–707. [PubMed: 18521104]

[24]. Hanahan D, Weinberg RA. Hallmarks of cancer: the next generation. Cell. 2011; 144:646–674. [PubMed: 21376230]

[25]. Levine AJ, Puzio-Kuter AM. The control of the metabolic switch in cancers by oncogenes and tumor suppressor genes. Science. 2010; 330:1340–1344. [PubMed: 21127244]

[26]. David CJ, Chen M, Assanah M, Canoll P, Manley JL. HnRNP proteins controlled by c-Myc deregulate pyruvate kinase mRNA splicing in cancer. Nature. 2010; 463:364–368. [PubMed: 20010808]

[27]. Mazurek S. Pyruvate kinase type M2: a key regulator of the metabolic budget system in tumor cells. Int J Biochem Cell Biol. 2011; 43:969–980. [PubMed: 20156581]

[28]. Christofk HR, Vander Heiden MG, Harris MH, Ramanathan A, Gerszten RE, Wei R, et al. The M2 splice isoform of pyruvate kinase is important for cancer metabolism and tumour growth. Nature. 2008; 452:230–233. [PubMed: 18337823]

[29]. Yang W, Xia Y, Ji H, Zheng Y, Liang J, Huang W, et al. Nuclear PKM2 regulates beta-catenin transactivation upon EGFR activation. Nature. 2011; 480:118–122. [PubMed: 22056988]

[30]. Luo W, Hu H, Chang R, Zhong J, Knabel M, O'Meally R, et al. Pyruvate kinase M2 is a PHD3-stimulated coactivator for hypoxia-inducible factor 1. Cell. 2011; 145:732–744. [PubMed: 21620138]

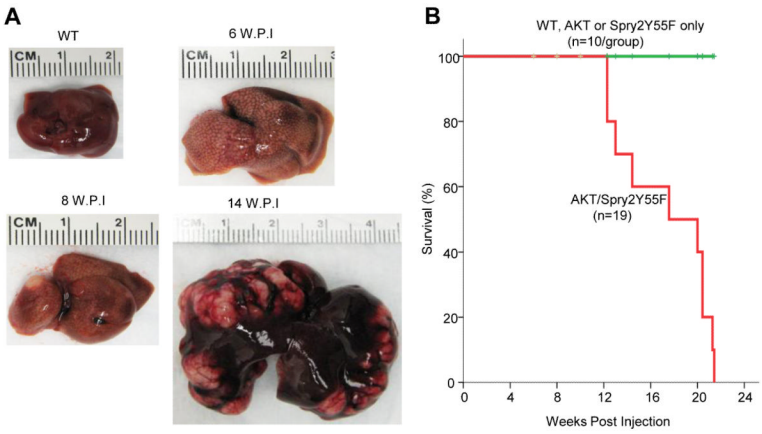

Fig. 1. Co-expression of Spry2Y55F and activated AKT induces liver tumor development in mice

(A) Macroscopic pictures of wild type (WT) and AKT/Spry2Y55F-injected mice livers at different time points. W.P.I: weeks post-injection. (B) Survival curve of the wild-type (WT), AKT only-, Spry2Y55F only- and AKT/Spry2Y55F-injected mice.

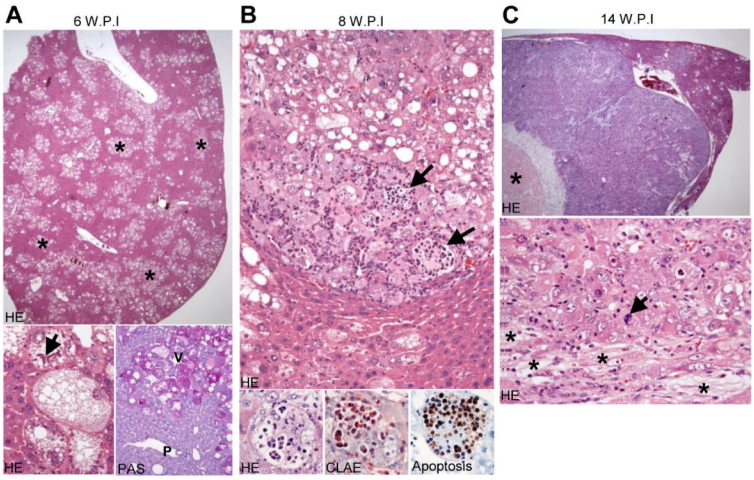

Fig. 2. Histological features of AKT/Spry2Y55F mice livers at different time points

(A) PAS: Periodic Acid-Schiff. V: hepatic vein; P: portal tract. The asterisk and arrow in marks some preneoplasias and a Mallory-Denk-body respectively. Magnification of upper HE stain: 20x; lower HE stain: 400x; PAS stain: 200x. (B) The arrows point to emperipolesis of neutrophil granulocytes. CLAE: chloracetate-esterase enzyme. Upper panel: 200x; lower three panels (oil immersion): 1000x. (C) The asterisk in the upper panel of marks necrosis. The asterisks and arrow in the lower panel mark fibrosis and a mitotic feature, respectively. Upper panel: 20x, lower panel: 400x.

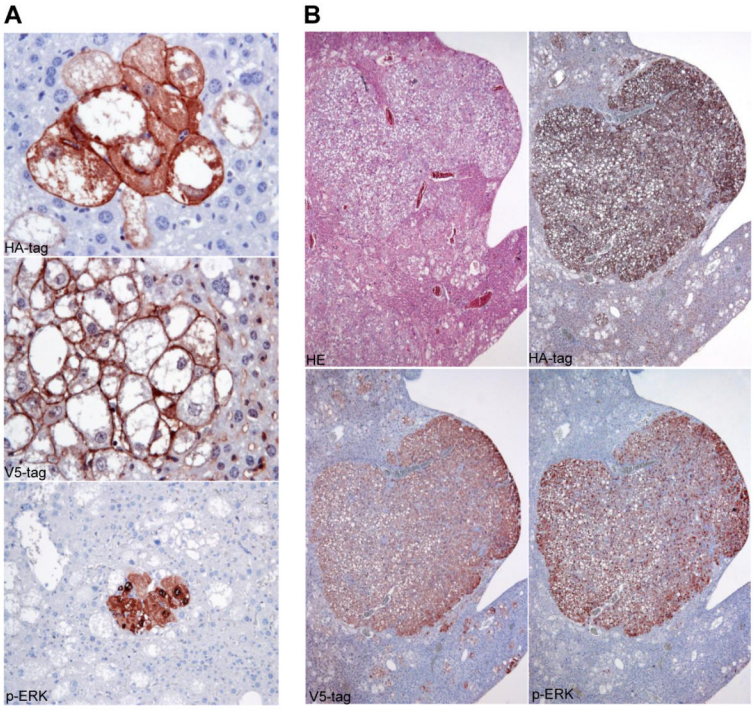

Fig. 3. Preneoplastic lesions and HCCs developed in AKT/Spry2Y55F mice express V5-Spry2Y55F, HA-AKT, and p-ERK

Immonohistochemical staining of V5-tag of Spry2Y55F, HA-tag of AKT, and p-ERK in (A) preneoplastic lesions and (B) a large HCC. Magnification of HA-tag and V5-tag staining in the preneoplasias: 400x; p-ERK in preneoplasias: 200x; tumor panels: 40x.

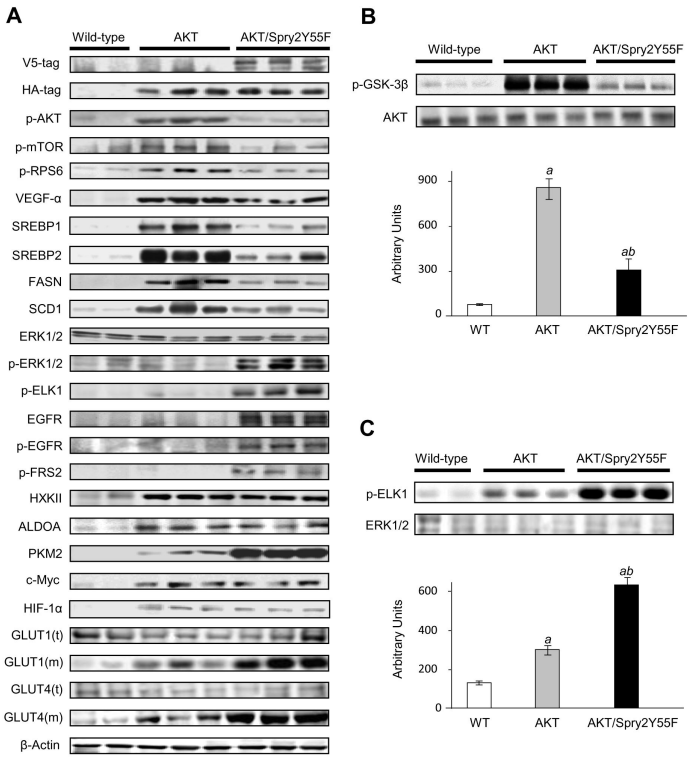

Fig. 4. MAPK pathway and PKM2 are upregulated in AKT/Spry2Y55F liver tumors

(A) Protein levels in WT livers, AKT and AKT/Spry2Y55F HCCs as analyzed by western blotting. *t:* total; *m:* membranous. (B) Kinase activity of AKT in WT livers, AKT and AKT/Spry2Y55F HCCs. (C) Kinase activity of MAPK in WT livers, AKT and AKT/Spry2Y55F HCCs. Six to ten samples per group per assay were analyzed. Each bar represents mean ± SD. Tukey-Kramer test: $P < 0.001$, *a*, vs. wild-type livers; *b*, vs. AKT HCCs; *c*, vs. AKT/Spry2Y55F HCCs.